Available online at www.sciencedirect.com
ScienceDirect
Mechanical Systems and Signal Processing 21 (2007) 1917–1926
Mechanical Systems and Signal Processing
www.elsevier.com/locate/jnlabr/ymssp

Third-order spectral characterization of acoustic emission signals in ring-type samples from steel pipes for the oil industry ☆

Juan José González de la Rosa[a,*], Rosa Piotrkowski[b], José Ruzzante[c]

[a]*University of Cádiz, Electronics Area, Research Group PAI-TIC-168: Computational Instrumentation and Industrial Electronics, EPSA, Avda. Ramón Puyol S/N, E-11202, Algeciras, Cádiz, Spain*
[b]*Comisión Nacional de Energía Atómica-Univ. Nac. de General San Martín, Avda. General Paz 1499, E-1650-San Martín, Buenos Aires, Argentina*
[c]*UTN-Regional Delta, Argentina*

Received 19 December 2005; received in revised form 3 June 2006; accepted 25 August 2006
Available online 10 October 2006

Abstract

Third-order cumulant spectra are used to characterize acoustic emission events in ring-type samples from steel pipes for the oil industry. A cut segment of chord allows the coupling between a sample and the mechanical excitation device. Diagonal bi-spectrum allows the separation of the primary (original) deformation from the reflections produced mainly in the suppressed chord. These longitudinal reflections can hardly be extracted via second-order methods, e.g. wavelet packets and power spectra, because they are partially masked by both Gaussian and non-Gaussian noise. Sample registers were acquired by wide frequency-range transducers (100–800 kHz) and digitalized by a 2.5 MHz, 8-bit ADC.

Keywords: Acoustic emission (AE); Bi-spectrum; Frequency domain analysis; Higher-order statistics (HOS); Non-destructive testing (NDT); Time-frequency analysis; Vibration analysis

1. Introduction

In AE signal processing we usually deal with the characterization and separation of multiple events which sequentially occur in localized measurement areas during a non-destructive test (NDT). In most situations, the primary burst resulting from an excitation, and the successive reflections at the internal or free surfaces (echoes) have to be monitored, because echoes often carry information associated with the medium through which they propagate, as well as with the reflecting surface's properties, as it was mentioned in [1]. The characterization consists of determining the time instants at which the echoes occur, along with their power spectra (*fingerprint*).

Although AE signals have distinctive time instances, it is difficult to detect them in a noisy environment. Furthermore, there is a limitation in the number of echoes which can be extracted, due to their low-level

☆This work reflects a multidisciplinary research of the Latin-American Elastic Waves Group (GLEA).

*Corresponding author. Tel.: +34 956028020; fax: +34 956028001.
E-mail address: juanjose.delarosa@uca.es (J.J. González de la Rosa).

0888-3270/$ - see front matter © 2006 Elsevier Ltd. All rights reserved.
doi:10.1016/j.ymssp.2006.08.011

amplitudes. A variety of signal processing methods have been used in similar situations and in other fields of Science and Technology [2–9]. They include statistical analysis, spectral analysis, time-frequency analysis (spectrogram) and wavelet transforms, and are based on the energy conservation hypothesis; so they are useful for finding predominant information, such as peaks. But low SNR sources cannot be identified successfully, because the algorithms retain energy information from one domain to another. As a consequence, transient signals of interest, like pulse-like events, may be buried in the background. Furthermore, non-Gaussian signals are not completely characterized up to second order. As a consequence, additional information should be found in the amplitude and phase charts of their higher-order statistics.

Different failure mechanisms produce AE events, whose analysis provide us with information regarding both the cause of the breaks and the media through which the vibratory waves propagate. An average complex AE event comprises different sub-events, stated as two chief classes. First, arrivals of successive events due to only one type of mechanism. A breakage which is getting bigger belongs to this set of complex events; when the burst bumps into an anchoring point, it gives rise to new different bursts or to a quite complex one, depending on the relationship between the arrival times of the simple bursts and the individual duration of the bursts. Secondly, there are also bursts which come from different sources, provoked by different types of mechanisms, e.g. formation or advancement of cracks, deformation, coating failure, corrosion, etc.

In the present paper we analyze results of a deformation test performed on ring-type samples coming from a steel pipe used in the oil industry. A chord of each ring was eliminated in order to introduce the sample in the deformation device. Both test and samples are designed so as the AE burst originates in the deformation of a specific region of the ring.

We study the main burst and the longitudinal reflections at the chord borders. But we also have the reflections which take place at the transversal borders of the pipe sample. These lateral or transversal strains comprise the main source of noise, which is desirable to be extracted. So we have the usual noise sources which come from the environment and the measurement equipment (usually Gaussian or uniform); but also have self-induced noise coming from the transversal reflections (in general non-Gaussian), masking the bursts originated in longitudinal reflections.

In this paper a bi-spectral analysis (the FFT of the third-order cumulants) is performed with a twofold purpose. First, to enhance the characterization of the AE longitudinal events over the measurement background noise (electronic noise usually symmetrically distributed). Secondly, to find out more reflections, which are masked by the transversal reflections (self-induced noise) with the same order of magnitude, and cannot be detected using power spectrum and wavelet packet analysis.

Thus, the new frequency components, discovered using HOS, are associated mainly to the reflections of the original deformation in the borders of the suppressed chord, which have been previously described in [10], and also to the transversal bursts. Whilst using second-order methods only two longitudinal reflections can be discovered, the averaged bi-spectrum of the signal records reveals two more.

We conclude that third-order spectra reveal two or three more echoes, which are supposed to be additional higher-order frequency components, which cannot be discovered using second-order methods. In this work, some (2–3) longitudinal reflections are depicted in the time-domain graphs, and can be identified by visual inspection because they are far enough from each other. However, transversal reflections may be hidden into the former ones, modifying the apparent duration. Then, we use higher-order spectra to find additional frequency components. Besides, in the case it is not possible to perform a visual separation of the longitudinal echoes, HOS would be specially welcome. The results can be applied in future work to characterize failure mechanisms of pipes for the oil industry.

The paper is structured as follows: in Section 2 we make a brief progress report on AE characterization; higher-order statistics are also defined, focusing on the indirect estimate of the bi-spectrum. Results are displayed in Section 3. Finally, conclusions and achievements are drawn in Section 4.

2. Higher-order statistics for AE signals characterization

High-order statistics, known as cumulants, are used to infer new properties about the data of non-Gaussian processes [7,11–13]. The relationship among the cumulants of r stochastic signals, $\{x_i\}_{i\in[1,r]}$, and their moments

of order $p, p \leqslant r$, can be calculated by using the *Leonov–Shiryayev* formula [11,12,14,15]:

$$Cum(x_1,\ldots,x_r) = \sum(-1)^k \times (k-1)! \times E\left\{\prod_{i\in v_1} x_i\right\} \times E\left\{\prod_{j\in v_2} x_j\right\} \cdots E\left\{\prod_{k\in v_p} x_k\right\}, \tag{1}$$

where the addition operator is extended over all the set of v_i $(1 \leqslant i \leqslant p \leqslant r)$ and v_i compose a partition of $1,\ldots,r$.

Let $\{x(t)\}$ be an rth-order stationary random process. The rth-order cumulant is defined as the joint rth-order cumulant of the random variables $x(t)$, $x(t+\tau_1),\ldots,x(t+\tau_{r-1})$,

$$C_{r,x}(\tau_1,\tau_2,\ldots,\tau_{r-1}) = Cum[x(t), x(t+\tau_1),\ldots,x(t+\tau_{r-1})]. \tag{2}$$

We assume in the following that the cumulant sequences satisfy the bounding condition:

$$\sum_{\tau_1=-\infty}^{\tau_1=+\infty} \cdots \sum_{\tau_{r-1}=-\infty}^{\tau_{r-1}=+\infty} |C_{r,x}(\tau_1,\tau_2,\ldots,\tau_{r-1})| < \infty. \tag{3}$$

Under this assumption, the higher-order spectra are usually defined in terms of the rth-order cumulants as their $(r-1)$-dimensional Fourier transforms, according to

$$S_{r,x}(f_1,f_2,\ldots,f_{r-1}) = \sum_{\tau_1=-\infty}^{\tau_1=+\infty} \cdots \sum_{\tau_{r-1}=-\infty}^{\tau_{r-1}=+\infty} C_{r,x}(\tau_1,\tau_2,\ldots,\tau_{r-1}) \exp[-j2\pi(f_1\tau_1 + f_2\tau_2 + \cdots + f_{r-1}\tau_{r-1})]. \tag{4}$$

The special poly-spectra derived from (4) are power spectrum ($r=2$), bi-spectrum ($r=3$) and tri-spectrum ($r=4$). Only power spectrum is real, the others are complex magnitudes. These multidimensional functions comprise a lot of information, and their computation may be impractical in some cases. To extract useful information one-dimensional slices [16–18] of cumulant sequences and spectra are usually used in non-Gaussian stationary processes.

The definition in Eq. (4) is based on the assumptions that an infinite sequence of higher-order statistics are available and known exactly [15]. In practice however, only a finite set of measurements is available. The conventional methods (FFT based) for estimation of higher-order spectra can be divided into three classes: the indirect class, which uses approximations of Eq. (4); the direct class, which may be based on the higher-order periodgram; and the complex demodulates class, which can be found summarized in [15].

Results have been obtained using indirect functions from MATLAB-HOSA toolbox [19]. Each function estimates first the higher-order statistics from a finite length sequence of data, and then calculates the higher-order spectral estimates using multidimensional windows functions [15].

Provided with the mathematical foundations the experimental results are presented hereinafter.

3. Experiments and results

3.1. Experimental arrangement, experiment design and second-order spectra analysis

The experimental arrangement is depicted in Fig. 1, where some relevant dimensions are indicated. It consists of a test ring (the sample) which is going to be under test. One sensor is attached to the outer surface of the ring-type sample, which is under mechanical excitation. The ring has an outer diameter of 138–140 mm, and is attached to the excitation device by a segment of chord of about 70 mm. A bending (near the sensor) in the inside upper face is thought to concentrate the elastic waves.

A number of 20 sequences were acquired using a wide-band sensor $PAC - WD$ (100–800 kHz). Each signal comprises 2502 points (sampling frequency of 2.5 MHz and 8 bits of resolution). Each time-series assembles the main AE event and the subsequent reflections (echoes).

At a first glance it is possible to distinguish 2 or 3 AE events in each signal. Fig. 2 shows an example of a time instance and its power spectrum.

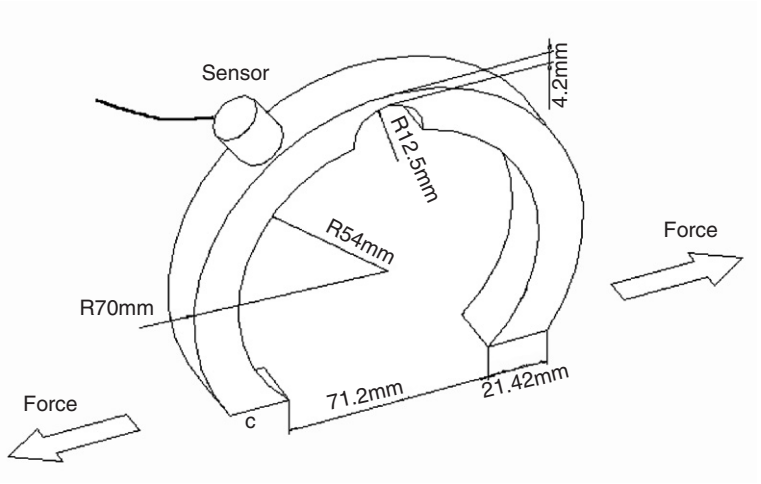

Fig. 1. Experimental arrangement.

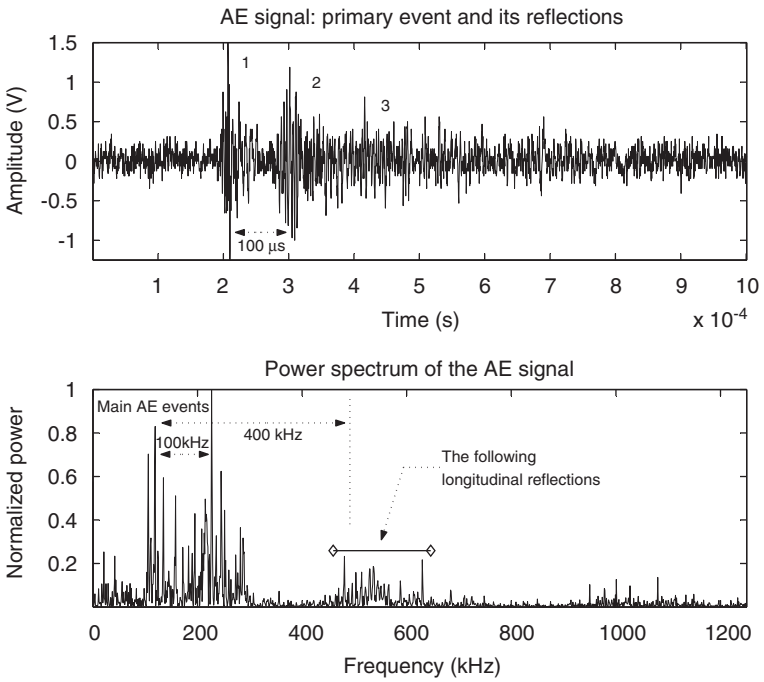

Fig. 2. An AE signal (up) and its spectrum (down).

The main frequency components in Fig. 2 are concentrated in the interval 0–300 kHz. It is difficult to distinguish the main AE event from the secondary events (reflections or echoes), both in the frequency and time domains. This is caused by two facts. On one side, the measurement system introduces a noise floor to the spectrum; this noise is in general symmetrically distributed. Another factor is the lack of information regarding the phase of the components. Power spectrum only gathers information from amplitudes of the different components.

Another relevant fact deals with the difficulty of selecting the main frequency components in the power spectrum. Fig. 3 reflects this fact. Apparently, all the frequency components are equally important. Frequencies that will be enhanced in higher-order spectra are marked with an arrow. In the second-order spectrum they are even less important than the other terms.

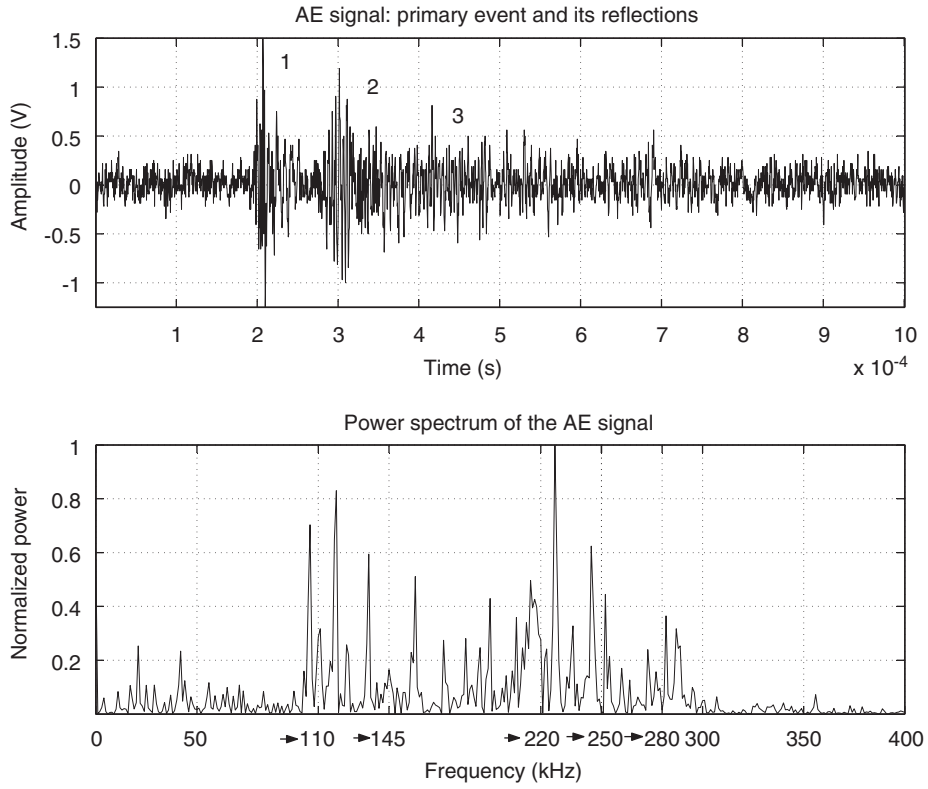

Fig. 3. A zoom of the spectrum shown in Fig. 2 which allows to observe the higher-order frequency components.

The de-noising procedure using wavelet packets was developed using a *sym*8, belonging to the family *Symlets* (order 8), which are compactly supported wavelets with least asymmetry and highest number of vanishing moments for a given support width. We also choose a soft heuristic thresholding. The same 20 sample (SNR $= 2$ dB) registers have been processed; in Fig. 4 we show the best result of the analysis. As the decomposition level increases no more reflections are found.

3.2. Third-order spectral characterization

In order to provide some further insight in the frequency domain, the third-order spectrum is calculated (an unbiased estimate is used). Fig. 5 shows the three-dimensional graph of the average diagonal bi-spectrum. The diagonal slice is selected as the main direction.

The data are non-stationary, so we follow the usual procedure for non-stationary mean value measurement, consisting of storing each record $x_i(t)$, as a function of t, $0 \leqslant t \leqslant T$ (T, is the measurement window). After this has been done for all the records, we perform an ensemble average [20].

Despite the fact that for non-stationary signals time-frequency distributions (that describe the temporal evolution of the spectrum or the poly-spectrum) are useful tools, in this case they do not outperform the ensemble averaging procedure. We compare results to the best result obtained with wavelet packets.

Fig. 6 shows the average diagonal bi-spectrum of the sequences. We can distinguish the main peak associated with the AE cause and the successive echoes' peaks, which have a decreasing amplitude and a frequency shift around the peak frequency (from left to right and *vice versa*). A maximum lag (time shift between samples) of 200 is assumed as the starting point of the resolution analysis.

To confirm the origin of the peaks and to gain resolution we are provided with Fig. 7. The upper graph is the bi-spectrum of the complete AE sequence, this time for a max lag of 1024. The graph in the middle shows the average bi-spectrum of the main AE event, without the echoes. The lowest sub-figure shows the

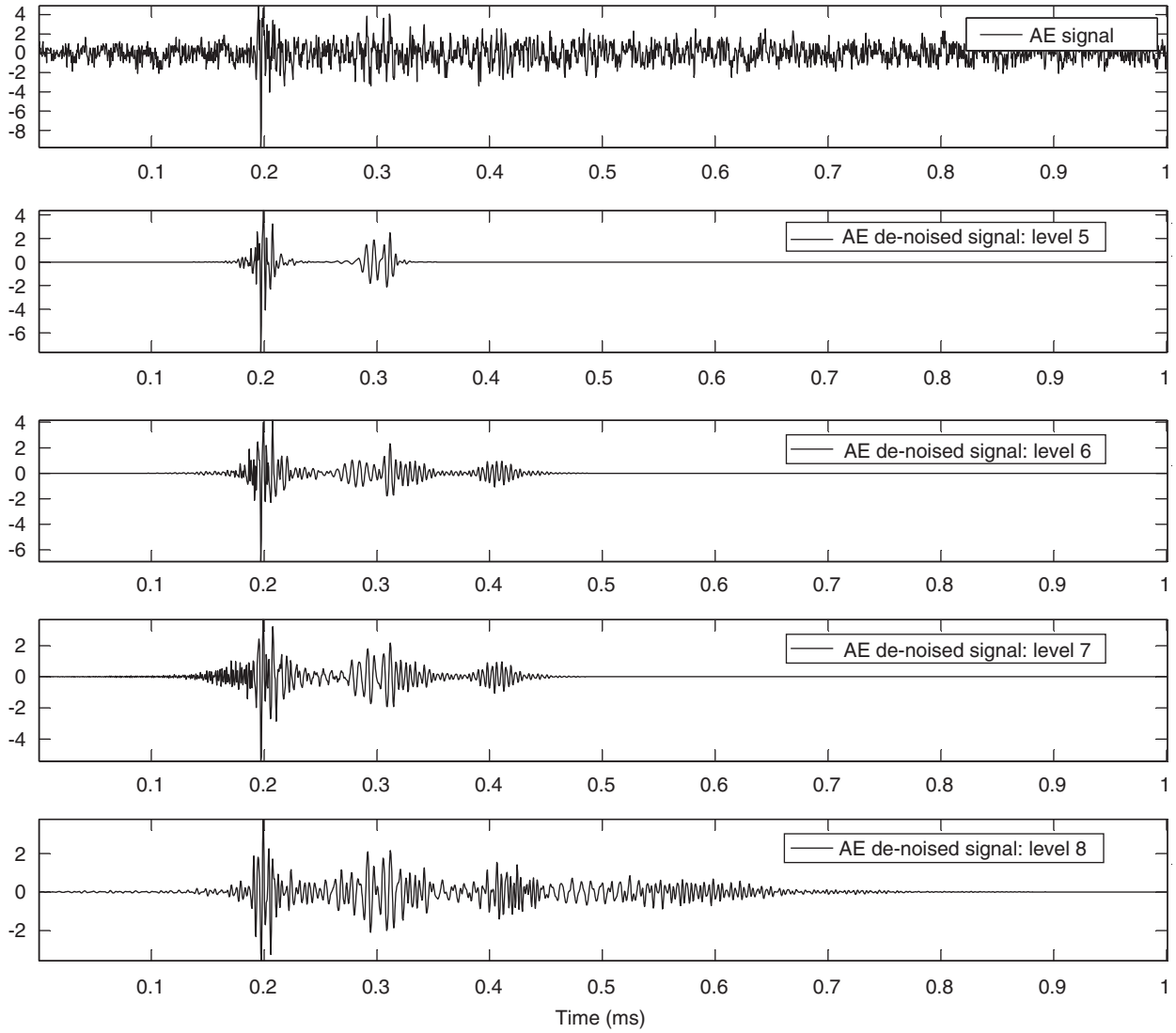

Fig. 4. The best result of the wavelet packets analysis. The primary burst and two reflections can be recovered.

bi-spectrum estimation of the reflections. We conclude the existence of a main AE event (connected with a perturbation), which takes the highest value at 145 kHz (roughly) and the secondary lower-amplitude echoes also characterized by a frequency shift.

Comparing graphs in Figs. 6 and 7 we can see the effects of improving the resolution in the frequency domain. The better the resolution, the higher the magnitude levels associated with relevant frequency components. This is due to the fact that non-Gaussian processes have been enhanced over symmetrically distributed ones, like the noise form the measurement equipment.

Another characterization of the main AE event is obtained from the contour plot of the average bi-spectrum of the complete AE event. Fig. 8 shows the contour of the bi-spectrum estimated via the indirect method.

The bi-spectrum displayed in Fig. 8 reveals the main region, distributed in the surroundings of the peak (0.1,0.1), which is connected with the main AE event; and the five other symmetric locations as indicated in [19]. The non-redundant region of support for the bi-spectrum is the triangle with vertices (0,0), (1/3,1/3) and (1/2,0); where we have assumed a normalized sampling frequency of 1 Hz [19].

We can guess that the non-Gaussian noise originates in transversal reflections. This can be sustained in some simple calculations based on orders of magnitude and on the Fig. 2. It is measured a $\Delta t = 100\,\mu s$ and a

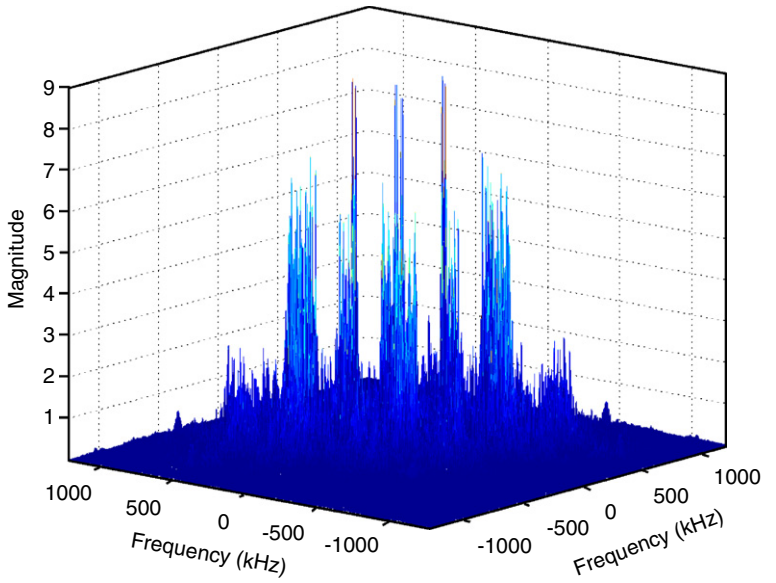

Fig. 5. Tri-dimensional representation of the magnitude of the diagonal bi-spectrum of the signal shown in Fig. 2.

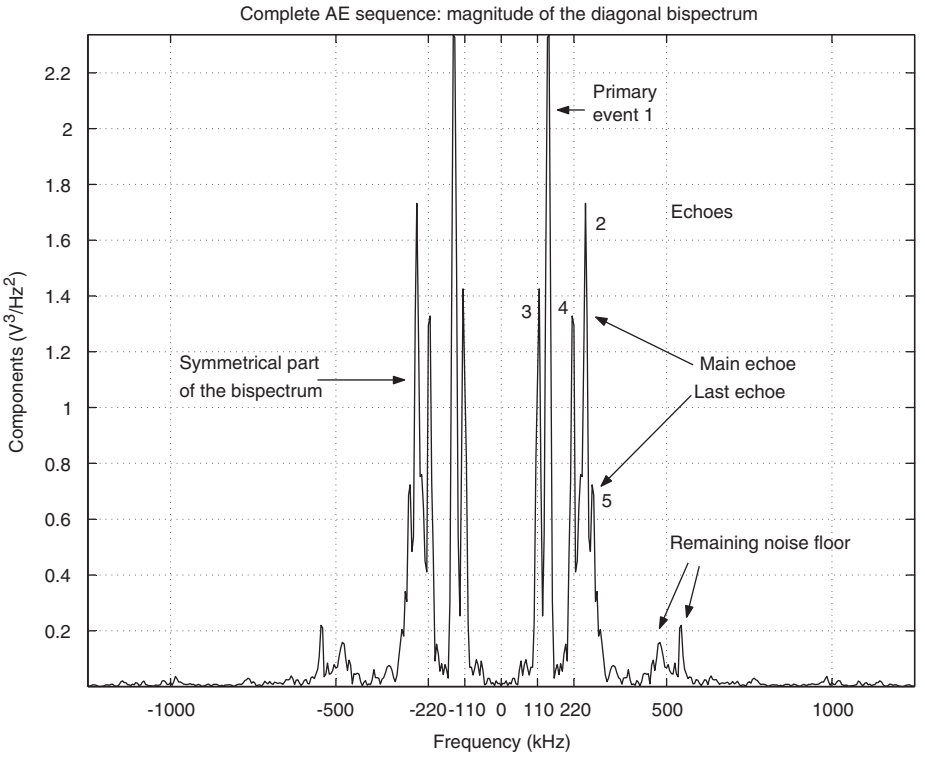

Fig. 6. Average diagonal bi-spectrum of the complete AE signals. 1: primary event. 2–5: echoes. Maximum lag of 200.

$\Delta f = 100\,\text{kHz}$, between the original event and the first reflection, in the time domain and in the frequency domain, respectively. Estimating, in the power spectrum diagram, a $\Delta f = 400\,\text{kHz}$ between the original event's peak and the location of the noise peak, we obtain a $\Delta t = 25\,\mu\text{s}$. Then, using a speed propagation value of the longitudinal waves in the steel of the order of 1 km/s [10] we find a distance of around 2 cm, which matches the

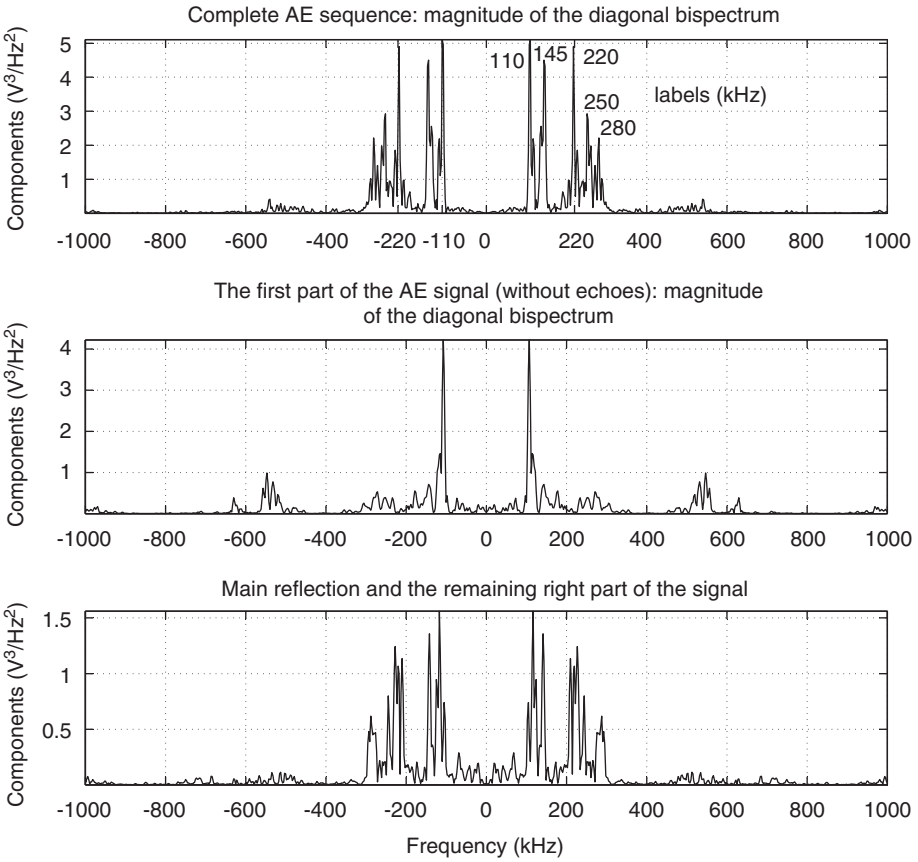

Fig. 7. The main AE event (up) and the rest of the AE event (down). Average diagonal bi-spectra.

transversal dimension of the ring sample. Thus, the mechanical non-Gaussian noise could be associated to the transversal reflections.

The above results lead us to some conclusions on the use of HOS as a characterizing and separating tool to be considered in a non-destructive measurement system.

4. Conclusions and accomplishments

The significance of this contribution lies in the fact of enhancing the characterization of the longitudinal AE events in the frequency domain. By one side, bi-spectral estimation of the signals reveals information regarding the reflecting surface of the pipeline sample the sensor is coupled to. Secondly, the experience takes benefits from the inherent advantages of HOS, regarding the extra information added to non-Gaussian processes and the enhancing of the SNR.

On the other hand, frequency components associated to the reflections could be used to get comprehensive information from the main AE (strain or stress or any other perturbation) and the non-linear echoes.

Finally, the mechanical noise is associated to the transversal reflections, which mask the duration of the longitudinal reflections, which are desirable to be extracted and characterized. What is more, third-order spectrum diagrams do not contain information regarding the symmetric noise, but they have information about these non-Gaussian additive transversal reflections.

Actually, we are working to propose tri-spectrum as a complementary tool, in order to confirm the presence of the higher-order components found in the diagonal bi-spectrum.

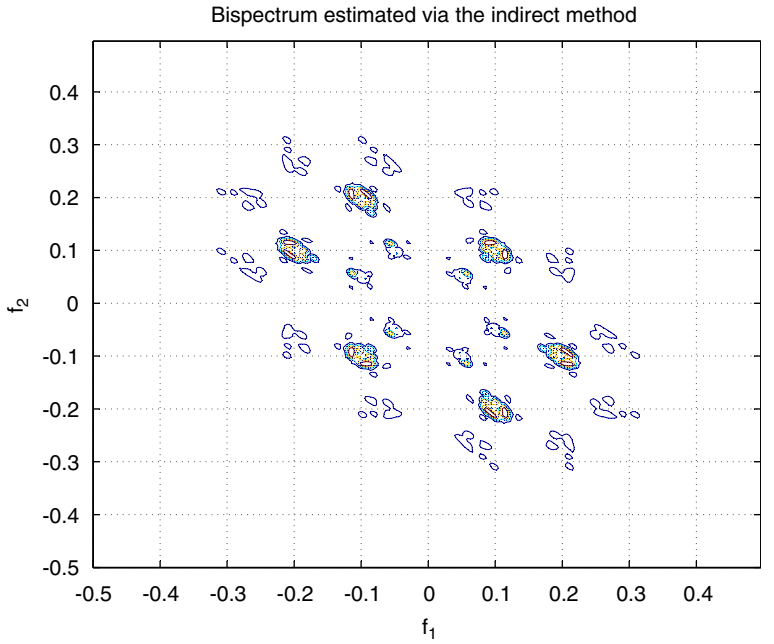

Fig. 8. Bi-spectrum of an AE signal estimated by the indirect method [19] for a max lag value of 64. A normalized sampling frequency of 1 Hz is assumed.

Acknowledgement

The authors would like to thank the *Spanish Ministry of Education and Science* for funding the project DPI2003-00878 which involves noise processes modeling and time-frequency calibration. Also would like to thank the Andalusian Government for funding the project TIC-155 which involves HOS applications.

References

[1] J.J.G. De la Rosa, I. Lloret, J. Ruzzante, R. Piotrkowski, M. Armeite, M.L. Pumarega, Higher-order characterization of acoustic emission signals, in: CIMSA 2005, Proceedings of the 2005 IEEE International Conference on Computational Intelligence for Measurement Systems and Applications, Robert Myers ed., ISBN 0-7803-9026-1; IEEE Catalog Number 05EX1037, Giardini Naxos, Italy, 20–22 July, 2005, pp. 296–300, paper CM5027, Oral Presentation in the Session 16 Advanced Signal Processing 2.

[2] A. Gallego, J.F. Gil, J.M. Vico, J.E. Ruzzante, R. Piotrkowski, Coating adherence in galvanized steel assessed by acoustic emission wavelet analysis, Scripta Materialia 52 (10) (2005) 1075–1080.

[3] A.M. Al-Ghamd, D. Mba, A comparative experimental study on the use of acoustic emission and vibration analysis for bearing defect identification and estimation of defect size, Mechanical Systems and Signal Processing 20 (7) (2006) 1537–1571.

[4] J.-H. Lee, M.-R. Lee, J.-T. Kim, V. Luk, Y.-H. Jung, A study of the characteristics of the acoustic emission signals for condition monitoring of check valves in nuclear power plants, Nuclear Engineering and Design 236 (13) (2006) 1411–1421.

[5] R. Piotrkowski, A. Gallego, E. Castro, M. García-Hernández, J. Ruzzante, Ti and Cr nitride coating/steel adherence assessed by acoustic emission wavelet analysis, Non Destructive Testing and Evaluation (NDT and E) International 8 (4) (2005) 260–267.

[6] J. Mieza, M. Oliveto, M.L. Pumarega, M. Armeite, J. Ruzzante, R. Piotrkowski, Identification of AE bursts by classification of physical and statistical parameters, in: 31st Annual Review of Progress in Quantitative Non-destructive Evaluation, Proceedings, vol. 1, Golden-Colorado, USA, 2004.

[7] M.J. Hinich, Detecting a transient signal by biespectral analysis, IEEE Transactions on Acoustics 38 (9) (1990) 1277–1283.

[8] L.E. Kinsler, A.R. Frey, A.B. Coppens, J.V. Sanders, Fundamentals of Acoustics, fourth ed., Wiley Series in Probability and Statistics, vol. 1, 1998.

[9] I.G. Scott, Basic Acoustic Emission, Routledge, New York, 1991.

[10] R. Piotrkowski, M.I.L. Pumarega, M. Armeite, J. Mieza, J.E. Ruzzante, Analysis of echoes in acoustic emission signals, in: Third Pan American Conference for Non-destructive Testing, Proceedings, J.E. Ruzzante Ed., vol. 1, Río de Janeiro-Brazil, 2003, pp. 1270–1275.

[11] C.L. Nykias, J.M. Mendel, Signal processing with higher-order spectra, IEEE Signal Processing Magazine (1993) 10–37.

[12] J.M. Mendel, Tutorial on higher-order statistics (spectra) in signal processing and system theory: theoretical results and some applications, Proceedings of the IEEE 79 (3) (1991) 278–305.
[13] A.K. Nandi, Blind Estimation using Higher-order Statistics, first ed., vol. 1, Kluwer Academic Publishers, Boston, 1999.
[14] J.J.G. De la Rosa, C.G. Puntonet, I. Lloret, An application of the independent component analysis to monitor acoustic emission signals generated by termite activity in wood, Measurement 37 (1) (2005) 63–76 available online 12 October 2004.
[15] C.L. Nikias, A.P. Petropulu, Higher-order spectra analysis, A Non-Linear Signal Processing Framework, Prentice-Hall, Englewood Cliffs, NJ, 1993.
[16] J. Jakubowski, K. Kwiatos, A. Chwaleba, S. Osowski, Higher order statistics and neural network for tremor recognition, IEEE Transactions on Biomedical Engineering 49 (2) (2002) 152–159.
[17] J.J.G. De la Rosa, I. Lloret, C.G. Puntonet, J.M. Górriz, Higher-order statistics to detect and characterise termite emissions, Electronics Letters 40 (20) (2004) 1316–1317.
[18] B.E.P. Jr, H.A. Ware, D.P. Wipf, W.R. Tompkins, B.R. Clark, E.C. Larson, Fault diagnosis using statistical change detection in the bispectral domain, Mechanical Systems and Signal Processing 14 (4) (2000) 561–570.
[19] A. Swami, J.M. Mendel, C.L. Nikias, Higher-order spectral analysis toolbox user's guide, 2001.
[20] J. Bendat, A. Piersol, Random Data–Analysis and Measurement Procedures, third ed., Wiley Series in Probability and Statistics, vol. 1, Wiley Interscience, New York, 2000.